

Scaling of cluster growth for coagulating active particles

Peet Cremer* and Hartmut Löwen

Institut für Theoretische Physik II: Weiche Materie, Heinrich-Heine-Universität Düsseldorf, D-40225 Düsseldorf, Germany

(Received 28 October 2013; revised manuscript received 13 January 2014; published 21 February 2014)

Cluster growth in a coagulating system of active particles (such as microswimmers in a solvent) is studied by theory and simulation. In contrast to passive systems, the net velocity of a cluster can have various scalings dependent on the propulsion mechanism and alignment of individual particles. Additionally, the persistence length of the cluster trajectory typically increases with size. As a consequence, a growing cluster collects neighboring particles in a very efficient way and thus amplifies its growth further. This results in unusual large growth exponents for the scaling of the cluster size with time and, for certain conditions, even leads to “explosive” cluster growth where the cluster becomes macroscopic in a finite amount of time.

DOI: [10.1103/PhysRevE.89.022307](https://doi.org/10.1103/PhysRevE.89.022307)

PACS number(s): 64.75.Xc, 82.70.Dd

I. INTRODUCTION

Phase separation of a homogeneous state into two distinct bulk phases is not only relevant for many technological processes but also constitutes a classical problem of nonequilibrium statistical mechanics [1–4]. For ordinary fluids and solids, the separation process is usually triggered by an initial fluctuation from which a critical nucleus arises. This initial cluster grows and ripens according to different scaling laws [5]. Typically, the extension of the cluster increases with a power law $R(t) \sim t^\alpha$ of time, where the exponent α depends on the growth process and the dimensionality d of the system. For ordinary (passive) systems, α varies in the range between $1/3$ and 1 [6]. More recently, both for mesoscopic colloidal suspensions [7] and for complex plasmas [8], the phase separation process has been studied by observing the individual particle trajectories, giving insight into the microscopic (i.e., particle-resolved) mechanisms of the separation process [9].

While the physics of the phase separation processes is by now well-studied and understood for inert, passive particles, there is recent work demonstrating that similar separation and clustering processes occur for an ensemble of microswimmers. The latter can be regarded as active particles in a solvent (experiencing a Stokes drag) with an internal propulsion mechanism. In fact, there are widely different realizations of such active particles, ranging from swimming bacteria to artificial self-propelled colloidal particles [10–12].

Basically, two different separation processes in active systems occur. First, clustering can be purely motility induced [13], such that it vanishes if the self-propulsion is removed as recently demonstrated [14–22]. The simplest variant is a swarm of self-propelled particles resulting in an overall moving cluster. Second, there is already phase separation in the unpropelled, passive system, which is then altered due to the drive. This was considered, e.g., for a self-propelled Lennard-Jones system with attractive particle interactions [23,24]. Attraction can hardly be avoided in metal-capped colloidal swimmers due to the mutual van der Waals forces [23]. However, for active particles, the dynamical evolution

of cluster growth, as characterized by a nontrivial growth exponent α , has only rarely been considered apart from very recent studies [18,25–28].

In this paper, phase separation is investigated in a situation where active particles irreversibly coagulate with each other on contact, resulting in a compact aggregate. Irreversible coagulation is well understood for passive particles [29–33] and the scaling of cluster size with time has been studied as well [34–36]. We show here that activity of particles enables qualitatively different and novel cluster growth behavior. Due to the self-propulsion, clusters perform a persistent random walk [37] in contrast to the typical diffusive motion of passive particles. This allows a cluster of active particles to effectively “sweep up” smaller clusters, which self-accelerates and amplifies cluster growth considerably further. Our theoretical analysis and computer simulation show that the cluster growth scaling exponent α cannot only be considerably larger for active particles than the known values for passive particles, but that there is even a scenario of “explosive” cluster growth. We refer to the term “explosion” if the cluster reaches macroscopic size in a finite amount of time. Such explosive behavior was found earlier in the context of gelation kinetics (see, e.g., Refs. [38–41]) and in phase separation in external fields, like gravity [42].

In detail, the growth exponent α depends on the scaling of the total propulsion force of a cluster with its size, the persistence of the cluster trajectory, and the dimension d . We present several cases for the scaling of the total propulsion force of a cluster, which is determined by the type of swimmer, the fraction of particles contributing to the propulsion and the alignment of particles. If the cluster is driven by aligned surface particles only, in $d = 3$ dimensions we find up to exponential growth. Uncorrelated contribution of all particles leads to algebraic growth with up to $\alpha = 2$. Finally, if all particles in the cluster propel the cluster in the same direction, “explosive” growth becomes possible. These results apply for the case that clusters possess a compact structure. Additionally, we also consider the case where the growing cluster is fractal and discuss briefly the scaling implications on the growth laws. All our predictions are verifiable in experiments for self-propelled particles with very strong van der Waals attraction, e.g., as prepared in Ref. [23], phoretic attraction [14], or dipolar interaction [43].

*pcremer@thphy.uni-duesseldorf.de

II. SCALING THEORY

We perform our scaling theory in a general d -dimensional space ($d = 2, 3$) and assume that self-propelled particles irreversibly coagulate and form clusters with N member particles and radius R_N such that $R_N \propto N^{1/d}$. In the following, we refer to N as the cluster size. The cluster formation process is described in a simplified way insofar as we consider compact clusters only and distinguish between different extreme cases. Once the particles contribute to the cluster, they stay fixed and their direction of self-propulsion (or orientation) is frozen. One may therefore distinguish two basic cases, one, where all orientations of cluster particles are completely uncorrelated and another where all directions are perfectly aligned. The first case occurs if the orientational reordering is frozen-in during coagulation (as realized for rough spheres) while the latter case arises if there is a considerable alignment interaction during the coagulation process (as realised for example for rod-like artificial swimmers or bacteria). The next basic distinction concerns the particles that really contribute to the overall self-propulsion of the cluster. Here we also discuss two extreme cases: either all cluster particles contribute in the same way or only particles at the cluster boundary contribute. The first case is realized for two-dimensional catalytic swimmers on a substrate that are embedded in a bulk liquid such that there is enough fuel all over the cluster. It also occurs for coagulation of passive colloidal particles in gravity [42]. The second case of cluster surface activity is realized for three-dimensional catalytic swimmers where a fuel-depletion zone is created inside the cluster that reduces the push of inside particles [44–46]. Moreover, catalytic swimmers move along the gradient of the chemical, which also results in surface activity of the growing cluster [44–46]. Surface cluster activity also occurs due to hydrodynamics for pushers and pullers. When swimming in a tight formation, the propulsion of particles can be canceled by the flow created by the swimmers behind them. Consequently, only the particles in the rear of the cluster contribute to the total propulsion force [47], which again scales with the surface of the cluster.

A single swimmer is propagated formally by an internal force [48], which is compensated by the Stokes drag at low Reynolds number resulting in a constant propagation velocity $v^{(0)}$. All these individual forces $\mathbf{F}^{(i)}$ ($i = 1, \dots, N$) add up to give the total force \mathbf{F}_N acting on the cluster of size N and putting it into motion with a velocity v_N . This force \mathbf{F}_N is balanced by the Stokes drag acting on the cluster, which scales in both $d = 3$ and $d = 2$ [49] as $F_N \propto v_N R_N$. This after all yields different scalings for $F_N \propto N^\beta$ with a nontrivial exponent β such that

$$v_N \sim F_N/R_N \sim N^{\beta-1/d}. \quad (1)$$

We now focus more on the individual forces $\mathbf{F}^{(i)}$ that constitute F_N . As discussed before, a fraction of the particles in a cluster can be rendered inactive, implying $\mathbf{F}^{(i)} = 0$ for all inactive particles. Apart from this we assume an additional overall reduction of the nonvanishing $\mathbf{F}^{(i)}$ with the cluster size. We describe this reduction by assuming a further scaling law $\mathbf{F}^{(i)} \propto N^\gamma$ with a general exponent γ . The exponent γ vanishes for pushers and pullers [47,50] and for surface-tension-driven self-propelled droplets [51–52]. However, there

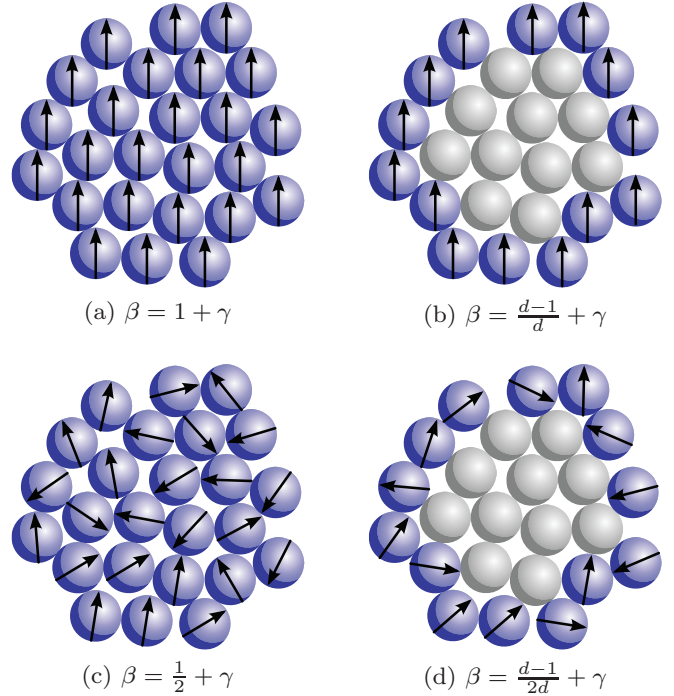


FIG. 1. (Color online) Four cases for the scaling exponent β of the total propulsion force F_N with cluster size N in d spatial dimensions. The arrows denote the directions of single-particle contribution forces.

are other situations where the effective individual forces $\mathbf{F}^{(i)}$ of contributing particles depend on the cluster size N , such that an overall reduction is relevant. Nontrivial values for γ can be estimated by relating the scaling of the velocity $v^{(0)}$ of an individual particle with its radius $R^{(0)}$ to the scaling of v_N with R_N via Eq. (1). Phoretic particles in $d = 3$ are propelled by a gradient generated on surface sites and their velocity is usually independent of the particle radius in three dimensions [46]. Ideally, the contributions of surface sites are aligned parallel and add up. Hence, $v_N \sim N^{(d-2)/d+\gamma}$ should not depend on $R_N \sim N^{1/d}$ in this situation, which yields $\gamma = -(d-2)/d$. Likewise, the velocity of phoretic particles in a fuel-scarce environment is known to depend inversely on the particle radius [45], implying $v_N \sim N^{-1/d}$ for aligned surface contributions and thus $\gamma = -(d-1)/d$.

Let us discuss the previously introduced four cases (see Fig. 1) in more detail. For each of the four cases, one can simply compute the exponent β for any prescribed γ as follows: We define a further exponent λ , which measures the particles contributing to the cluster propulsion such that $F_N \sim N^\lambda F^{(i)} \sim N^\lambda N^\gamma$. Insertion into Eq. (1) yields $\beta = \lambda + \gamma$. Contribution of all particles in case (a) means that $\lambda = 1$, while the case (b) where only surface particles contribute corresponds to $\lambda = \frac{d-1}{d}$. Random alignment of the particles imposes a factor $1/2$ leading to $\lambda = 1/2$ in case (c) and $\lambda = \frac{d-1}{2d}$ in case (d). These exponents are included in Fig. 1.

We now introduce a simple *sweeping argument* for active particles leading to scaling laws for the cluster size as a function of time t . Consider a typical cluster of size N traveling through the system that has a uniform number density $\bar{\rho}$ of

particles on average, no matter whether they are members of small clusters or noncoagulated, individual particles. Therefore, any inhomogeneities and local fluctuations in the particle and cluster distribution are neglected [53]. If $V(t)$ denotes the volume in d -dimensional space, which is covered by a cluster of size R_N moving with velocity v_N during a time t , we assume that all individual particles in this volume are irreversibly swept by the cluster. Differentially in time this implies

$$\frac{dN}{dt} = \bar{\rho} \frac{dV}{dt}. \quad (2)$$

Two limiting cases can be discriminated. In the so-called *ballistic* regime, the persistence is so high that the cluster trajectory appears straight on the length scale the cluster possesses itself such that the rate of the swept volume is $\frac{dV}{dt} \propto v_N R_N^{d-1} \sim N^{(d-2)/d+\beta}$. This will occur in any case if the cluster becomes so large that rotational diffusion is suppressed [54,55]. In the complementary case the cluster moves *diffusively*. Then the effective diffusion constant of a random walk with step velocity v_N scales as $D_N \sim v_N^2 \sim N^{2\beta-2/d}$, such that the volume swept out is given by [56] $\frac{dV}{dt} \sim R_N^{d-2} D_N \sim N^{(d-4)/d+2\beta}$. Insertion into Eq. (2) yields ordinary differential equations for $N(t)$ leading to our main result:

$$N(t) = \begin{cases} [N_0^{2/d-\beta} + C(2/d - \beta)t]^{1/(2/d-\beta)} & \beta < 2/d, \\ N_0 \exp(Ct) & \beta = 2/d, \\ C(\beta - 2/d)(t_c - t)^{-1/(2/d-\beta)} & \beta > 2/d, \end{cases} \quad (3)$$

for the *ballistic* regime, and

$$N(t) = \begin{cases} [N_0^{4/d-2\beta} + C(4/d - 2\beta)t]^{1/(4/d-2\beta)} & \beta < 2/d, \\ N_0 \exp(Ct) & \beta = 2/d, \end{cases} \quad (4)$$

for the *diffusive* regime, where $N_0 = N(t=0)$ is the initial cluster size and C is a positive amplitude prefactor. The last case of Eq. (3) corresponds to an explosive growth scenario, where the cluster size diverges after a finite time $t_c = \frac{N_0^{2/d-\beta}}{C(\beta-2/d)}$. Please note that $\beta > 2/d$ is never realized in the diffusive regime, as the cluster size would explode, which necessarily puts the system into the ballistic regime. When measuring size in terms of the cluster radius the algebraic growth exponents of $R(t) \propto t^\alpha$ are given by $\alpha = \frac{1}{2-\beta d}$ in the ballistic regime and $\alpha = \frac{1}{4-2\beta d}$ in the diffusive regime, which can be very large when βd is close to but below 2.

III. SIMULATION

Using computer simulation, we investigate the cluster growth for various values of β and different persistence lengths of cluster trajectories. The scaling of the total cluster force with an exponent β from Eq. (1) is an input in the simulation. Nevertheless, the final scaling of the cluster size with time as predicted by Eqs. (3) and (4) is not an input but an output. Therefore, this final scaling behavior is tested by our simulations. Moreover, the crossover to a possible ultimate scaling for *finite* clusters can be addressed and computed in a simulation.

In detail, the particles and compact clusters in these simulations are modeled as spherical droplets with radius

$R_N = R^{(0)} N^{1/d}$, so that the total volume of all member particles is conserved. Initially, single particles start at random positions in a periodic simulation box with velocity $v^{(0)}$ and random direction. Particle collision events are predicted and on contact, particles merge at their center of mass, forming larger clusters, which again merge when colliding. The velocity of clusters is assigned to $v_N = v^{(0)} N^{\beta-1/d}$. To model changes in the traveling direction of clusters in a general way, we use the following approach. After a reorientation time step Δt , a deviation from the current cluster direction is sampled for each member particle and the new cluster direction is taken as the average of all the member particle deviations. Then the collision events for the new time step are predicted. When two clusters merge, we weight each cluster with its number of member particles in the direction of the merged cluster. Since the averaging process is a biased random walk, the persistence length of cluster trajectories increases with cluster size N . We sample the direction deviations of each particle from a von Mises-Fisher distribution [57] with concentration parameter κ , which is used as an input parameter. This distribution plays the role of the normal distribution on the d -dimensional unit sphere and κ is similar to an inverse variance and determines the persistence of the trajectories such that we refer to κ as the persistence parameter in the following. Both the ballistic and diffusive regime can be gained as extreme limits $\kappa \rightarrow \infty$ or $\kappa = 0$.

The single-particle radius $R^{(0)}$ defines the length scale in the system, while the time $\tau = R^{(0)}/v^{(0)}$ a single-particle requires to travel its own radius is used as time scale. We

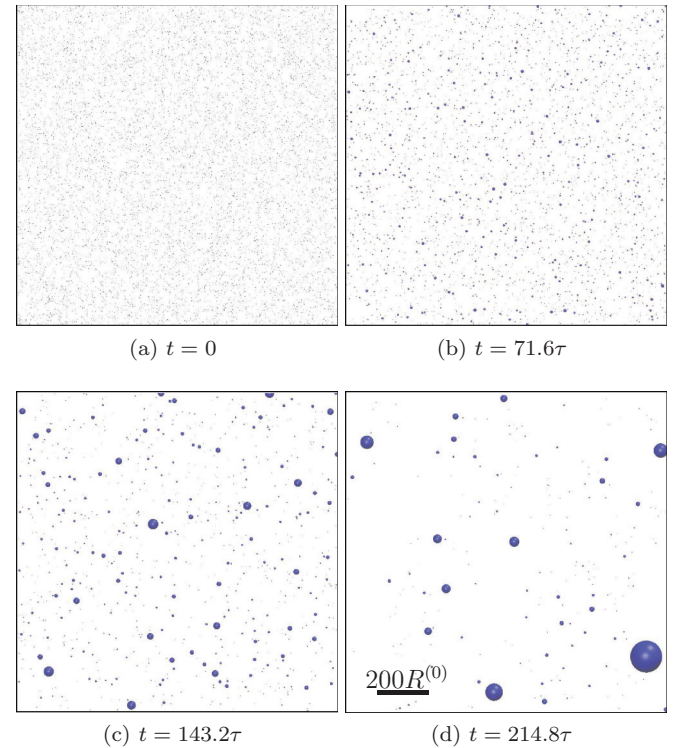


FIG. 2. (Color online) Typical simulation snapshots at various times, here in a two-dimensional simulation of $\mathcal{N} = 10^4$ total particles at packing fraction $\eta = 0.02$ with $\beta = 1$ and persistence parameter $\kappa = 100$. Snapshot (d) shows the situation just before the simulation is terminated.

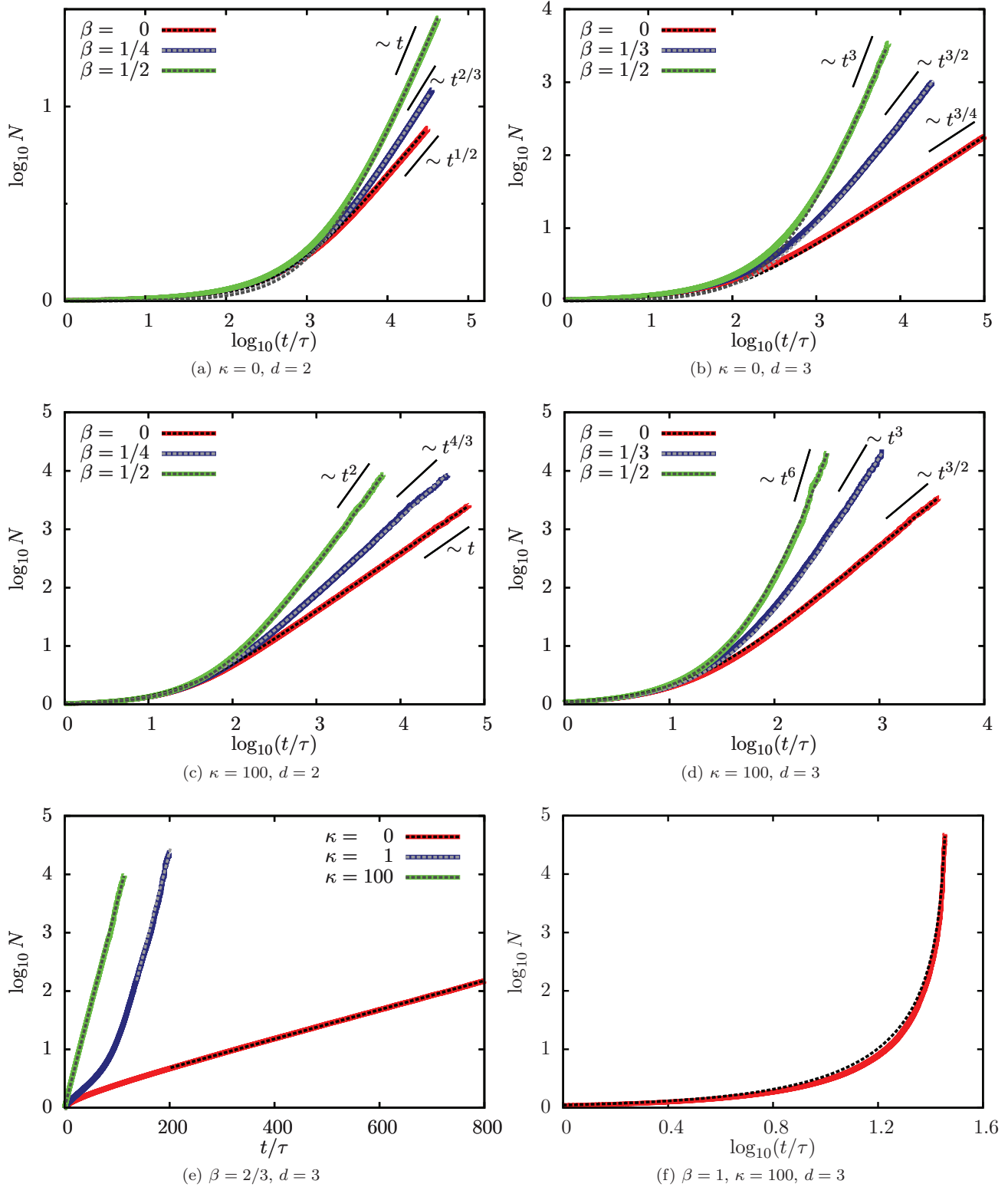


FIG. 3. (Color online) Cluster size evolution obtained from simulations in $d = 2, 3$ dimensions with various values of the persistence parameter κ and the total propulsion force scaling exponent β . Algebraic growth in the diffusive regime [(a), (b)] as well as in the ballistic regime [(c), (d)] occurs with the predicted exponents as indicated in the plots. Exponential growth (e) in the ballistic regime occurs faster than in the diffusive regime as indicated by the much higher slope. For high persistence and high force scaling, explosive cluster growth occurs (f). The dashed lines are fits using Eqs. (3) and (4), respectively.

chose $\Delta t = 0.1\tau$, which is sufficiently small when using a collision event prediction scheme. The packing fraction is taken as $\eta = 0.02$ with $\mathcal{N} = 10^6$ initial particles. We vary the scaling exponent β of the total propulsion force as well as the persistence parameter κ in $d = 2, 3$ dimensions. Since at late times the system is depleted of particles and the anticipated scaling laws clearly cannot be observed any more, we terminate the simulation as soon as a cluster reaches a size of $R_N > 0.05L$, where L is the box length. Typical snapshots from a simulation are shown in Fig. 2.

Figures 3(a) and 3(b) show the evolution of the mean cluster size $N(t)$ in two- and three-dimensional simulations in the diffusive regime ($\kappa = 0$) for various values of $\beta < 2/d$. Fits of $N(t)$ with Eq. (4) possess the predicted algebraic scaling. Data in the ballistic regime are shown in Figs. 3(c) and 3(d). The predicted scaling exponent for the algebraic growth is verified for all values of β .

For the case of $\beta = 2/d$, the predicted exponential growth in both regimes is reproduced by the simulations, and the prefactor C in the ballistic regime is significantly larger than in the diffusive regime; see the slope of the semilogarithmic plots in Fig. 3(e). The slope of the plot for $\kappa = 1$ steadily increases until it reaches the level for $\kappa = 100$ as clusters in this system need to grow first to enter the ballistic regime. Finally, for $\beta > 2/3$ in three dimensions explosive cluster growth is documented in Fig. 3(f), which confirms the predicted scaling $\sim (t_c - t)^{-3}$.

IV. FRACTAL AGGREGATES

Our results can be further extended to clusters that lack the reorganization mechanism leading to a compact shape. When particles and clusters simply stick to each other on the first point of contact, the resulting shapes possess a ramified and fractal structure [29,32].

The size of such aggregates can be conveniently described by the radius of gyration $R_N^{(g)}$, which replaces R_N and is approximately proportional to the hydrodynamic radius $R_N^{(h)}$ [58,59]. A structure with fractal dimension d_F ($1 \leq d_F \leq d$) then implies the scaling $R_N^{(g)} \sim N^{1/d_F}$. Therefore, the analog to Eq. (1) for fractal clusters is

$$v_N \sim F_N / R_N^{(h)} \sim F_N / R_N^{(g)} \sim N^{\beta-1/d_F}. \quad (5)$$

We have performed additional simulations implementing irreversible sticking of particles at the point of contact. Equation (5) is taken into account by assigning the cluster velocity to $v_N = v^{(0)}N^\beta/R_N^{(g)}$. Therefore, the radius of gyration of each cluster has to be tracked throughout the simulation. Apart from this, the simulation follows the same procedure as in Sec. III. Figure 4 shows typical snapshots confirming the ramified structure of the aggregates. We have determined the fractal dimension d_F from the simulation data for the cluster structure. Results for d_F are presented in the legends of Fig. 5.

In addition to the drag, the radius of gyration also determines the collision cross-section of the cluster. Applying the same simple sweeping argument used in Sec. II, we obtain $\frac{dV}{dt} \propto v_N R_N^{(g)d-1} \sim N^{(d-2)/d_F+\beta}$ for the rate of the

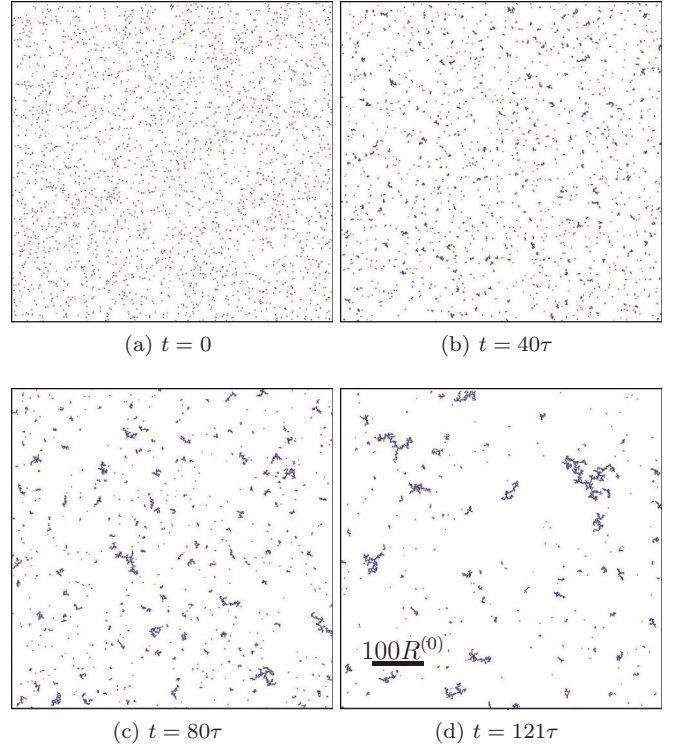


FIG. 4. (Color online) Typical snapshots of a two-dimensional simulation of fractal clustering using the same parameters as described in the legend of Fig. 2, except for the persistence parameter κ , which is now chosen to be $\kappa = 10$.

swept volume in the ballistic regime and $\frac{dV}{dt} \sim R_N^{(g)d-2} D_N \sim N^{(d-4)/d_F+2\beta}$ in the diffusive regime. Obviously, the sweeping volumes of compact clusters are recovered when setting $d_F = d$. Insertion into Eq. (2) then yields the scaling relations

$$N(t) = \begin{cases} [N_0^{\xi_b-\beta} + C(\xi_b - \beta)t]^{\frac{1}{\xi_b-\beta}} & \beta < \xi_b, \\ N_0 \exp(Ct) & \beta = \xi_b, \\ C(\beta - \xi_b)(t_c - t)^{\frac{-1}{\xi_b-\beta}} & \beta > \xi_b, \end{cases} \quad (6)$$

for the *ballistic* regime where the abbreviation $\xi_b = (2 - d)/d_F + 1$ is used. The critical time for explosive growth is $t_c = \frac{N_0^{\xi_b-\beta}}{C(\beta-\xi_b)}$ here. Note that for $d = 2$ these results are indistinguishable from Eq. (3) as ξ_b does not depend on d_F for $d = 2$.

For the *diffusive* regime we obtain the scaling law

$$N(t) = \begin{cases} [N_0^{\xi_d-2\beta} + C(\xi_d - 2\beta)t]^{\frac{1}{\xi_d-2\beta}} & \beta < \xi_d/2, \\ N_0 \exp(Ct) & \beta = \xi_d/2, \end{cases} \quad (7)$$

with $\xi_d = (4 - d)/d_F + 1$. Contrary to the behavior in the ballistic regime, the threshold value for β corresponding to exponential growth is raised as compared to compact clusters. Similarly, the algebraic growth exponents are lower for the same value of β .

Computer simulation results verifying the growth behavior for $d = 2$ in the ballistic regime are shown in Fig. 5(a) for the case of algebraic growth as well as in Fig. 5(b) for exponential growth. In fact, for $d = 2$, the algebraic growth exponents

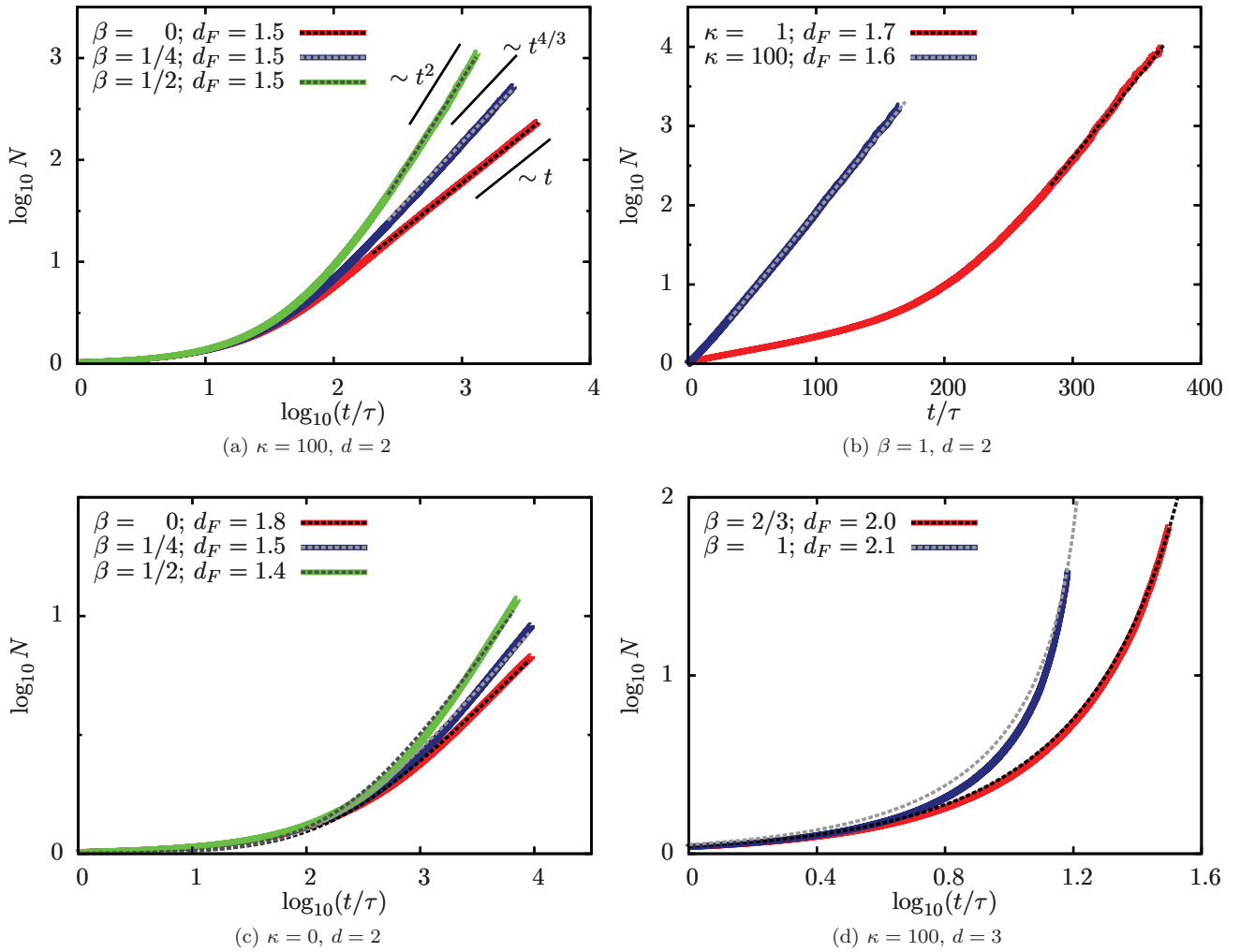


FIG. 5. (Color online) Fractal cluster-size evolution obtained from simulations in $d = 2, 3$ dimensions with various values of the persistence parameter κ and the total propulsion force scaling exponent β . For $d = 2$ in the ballistic regime (a), the same scaling laws hold as in the compact case. Accordingly, the threshold for exponential growth in the ballistic regime (b) remains at $\beta = 1$. In the diffusive regime for $d = 2$ (c) the fractal dimension d_F enters the scaling laws and leads to slower growth as compared to the compact case. Thresholds in β for explosive growth are lower for $d_F < d$ so that such growth behavior occurs already for $\beta = 2/3$ when $d = 3$ (d). The dashed lines are fits using Eqs. (6) and (7), respectively.

and the threshold for exponential growth are the same as in the compact case. Conversely, for $d = 3$, Fig. 5(d) shows explosive growth at high persistence not only for $\beta = 1$ but also for $\beta = 2/3$, confirming the reduced threshold. Finally, the prediction that the algebraic growth exponents in the diffusive regime are lower than in the compact case due to the influence of the fractal dimension is confirmed in Fig. 5(c), where results for algebraic scaling in the diffusive regime for $d = 2$ are shown.

V. CONCLUSIONS

In conclusion, we have investigated the scaling of cluster size with time for active particles in a solvent that irreversibly coagulate on collision by using theory and simulation. The scaling laws heavily depend on the scaling exponent β of the total propulsion force of clusters. We identify four main scenarios for the total propulsion force scaling. If all particles in a cluster are aligned and able to contribute, the fastest growth is possible. Completely uncorrelated directions of

particles lead to a significantly weaker scaling. Furthermore, hydrodynamics, fuel scarcity, or lack of a field gradient required for propulsion can lead to the situation that only particles on the surface of a cluster can contribute. These contributing particles can again be completely aligned or their directions can be completely uncorrelated. The scaling of the total propulsion force is then further modified by the details of the propulsion mechanism and the thereby implied scaling exponent γ of the single-particle contribution force with the size of the cluster.

Another crucial ingredient is the persistence length of cluster trajectories. In the diffusive regime, the persistence length is much smaller than the extension of clusters. Clusters explore the system volume and encounter each other on a diffusive time scale. More efficient growth occurs in the ballistic regime applying for a persistence length much larger than the cluster extension, where clusters sweep through the system volume on their semiballistic trajectories. The ballistic regime should be more relevant for active particle clusters

since the persistence length of trajectories of active particles is usually rather large and tends to increase with aggregate size.

We have verified these predictions in a simulation of compact clusters modeled as droplets that merge on contact in $d = 2, 3$ dimensions. The simulation data shows good agreement with the model scaling laws and gives the correct algebraic growth exponents or exponential growth corresponding to the various values of β in both regimes.

Additionally, we extended our model to fractal clusters that show a different growth behavior due to increased drag (hampering growth) and increased collision cross-section (enhancing growth). In the ballistic regime, the increased collision cross-section dominates the increased drag, leading to faster growth. However, in the diffusive regime, the increased drag dominates, resulting in a comparatively slower growth.

Given a sufficiently strong attraction between particles leading to irreversible coagulation, our findings are verifiable in experiments [14,23,43]. Usually it is attempted to avoid attractions like van der Waals attraction appearing in metal-capped active particles. However, by intentionally enhancing the attraction to a level where particles cluster irreversibly the prerequisites of our theory can be met.

ACKNOWLEDGMENTS

We thank Kurt Binder, Thomas Speck, Akira Onuki, and Hajime Tanaka for helpful discussions. Financial support from the ERC Advanced Grant INTERCOCOS (Grant No. 267499) and the DFG Science Priority Program SPP 1726 is gratefully acknowledged.

-
- [1] K. Binder and D. Stauffer, *Adv. Phys.* **25**, 343 (1976).
 [2] A. Onuki, *Phase Transition Dynamics* (Cambridge University Press, Cambridge, 2002).
 [3] H. Tanaka, *J. Phys.: Condens. Matter* **12**, R207 (2000).
 [4] H. Löwen, *Physica A* **235**, 129 (1997).
 [5] J. Krug, *Adv. Phys.* **46**, 139 (1997).
 [6] A. J. Bray, *Adv. Phys.* **51**, 481 (2002).
 [7] D. G. A. L. Aarts, R. P. Dullens, and H. N. W. Lekkerkerker, *New J. Phys.* **7**, 40 (2005).
 [8] A. Wysocki, C. R ath, A. V. Ivlev, K. R. S utterlin, H. M. Thomas, S. Khrapak, S. Zhdanov, V. E. Fortov, A. M. Lipaev, V. I. Molotkov, O. F. Petrov, H. L owen, and G. E. Morfill, *Phys. Rev. Lett.* **105**, 045001 (2010).
 [9] A. Ivlev, H. L owen, G. Morfill, and C. P. Royall, *Complex Plasmas and Colloidal Dispersions* (World Scientific, Singapore, 2012).
 [10] T. Vicsek and A. Zafeiris, *Phys. Rep.* **517**, 71 (2012).
 [11] P. Romanczuk, M. B ar, W. Ebeling, B. Lindner, and L. Schimansky-Geier, *Eur. Phys. J. Spec. Top.* **202**, 1 (2012).
 [12] M. E. Cates, *Rep. Prog. Phys.* **75**, 042601 (2012).
 [13] M. E. Cates and J. Tailleur, *Europhys. Lett.* **101**, 20010 (2013).
 [14] J. Palacci, S. Sacanna, A. P. Steinberg, D. J. Pine, and P. M. Chaikin, *Science* **339**, 936 (2013).
 [15] F. Peruani, A. Deutsch, and M. B ar, *Phys. Rev. E* **74**, 030904 (2006).
 [16] T. Ishikawa and T. J. Pedley, *Phys. Rev. Lett.* **100**, 088103 (2008).
 [17] H. H. Wensink and H. L owen, *Phys. Rev. E* **78**, 031409 (2008).
 [18] G. S. Redner, M. F. Hagan, and A. Baskaran, *Phys. Rev. Lett.* **110**, 055701 (2013).
 [19] I. Buttinoni, J. Bialk e, F. K ummel, H. L owen, C. Bechinger, and T. Speck, *Phys. Rev. Lett.* **110**, 238301 (2013).
 [20] J. Bialk e, H. L owen, and T. Speck, *Europhys. Lett.* **103**, 30008 (2013).
 [21] Y. Fily and M. C. Marchetti, *Phys. Rev. Lett.* **108**, 235702 (2012).
 [22] Y. Yang, J. Elgeti, and G. Gompper, *Phys. Rev. E* **78**, 061903 (2008).
 [23] I. Theurkauff, C. Cottin-Bizonne, J. Palacci, C. Ybert, and L. Bocquet, *Phys. Rev. Lett.* **108**, 268303 (2012).
 [24] G. Gr egoire, H. Chat e, and Y. Tu, *Physica D* **181**, 157 (2003).
 [25] G. S. Redner, A. Baskaran, and M. F. Hagan, *Phys. Rev. E* **88**, 012305 (2013).
 [26] A. Wysocki, R. G. Winkler, and G. Gompper, [arXiv:1308.6423v3](https://arxiv.org/abs/1308.6423v3) (2013).
 [27] E. M ehes, E. Mones, V. N emeth, and T. Vicsek, *PLoS ONE* **7**, e31711 (2012).
 [28] F. Peruani and M. B ar, *New J. Phys.* **15**, 065009 (2013).
 [29] P. Meakin, *Phys. Rev. A* **29**, 997 (1984).
 [30] P. Meakin, H. E. Stanley, A. Coniglio, and T. A. Witten, *Phys. Rev. A* **32**, 2364 (1985).
 [31] P. Meakin, T. Vicsek, and F. Family, *Phys. Rev. B* **31**, 564 (1985).
 [32] M. Kolb, R. Botet, and R. Jullien, *Phys. Rev. Lett.* **51**, 1123 (1983).
 [33] P. Meakin, A. Coniglio, H. E. Stanley, and T. A. Witten, *Phys. Rev. A* **34**, 3325 (1986).
 [34] E. Trizac and J.-P. Hansen, *J. Stat. Phys.* **82**, 1345 (1996).
 [35] G. F. Carnevale, Y. Pomeau, and W. R. Young, *Phys. Rev. Lett.* **64**, 2913 (1990).
 [36] M. Kolb, *Phys. Rev. Lett.* **53**, 1653 (1984).
 [37] R. Soto and R. Golestanian, *Phys. Rev. E* **89**, 012706 (2014).
 [38] E. Ben-Naim and P. L. Krapivsky, *Phys. Rev. E* **68**, 031104 (2003).
 [39] M. Herrero, J. J. L. Vel azquez, and D. Wrzosek, *Physica D* **141**, 221 (2000).
 [40] P. Singh and G. J. Rodgers, *J. Phys. A: Math. Gen.* **29**, 437 (1996).
 [41] P. Dongen and M. Ernst, *J. Stat. Phys.* **50**, 295 (1988).
 [42] G. Falkovich, A. Fouxon, and M. G. Stepanov, *Nature* **419**, 151 (2002).
 [43] L. Baraban, R. Streubel, D. Makarov, L. Han, D. Karnauschenko, O. G. Schmidt, and G. Cuniberti, *ACS Nano* **7**, 1360 (2013).
 [44] W. F. Paxton, K. C. Kistler, C. C. Olmeda, A. Sen, S. K. St. Angelo, Y. Cao, T. E. Mallouk, P. E. Lammert, and V. H. Crespi, *J. Am. Chem. Soc.* **126**, 13424 (2004).
 [45] S. Ebbens, M.-H. Tu, J. R. Howse, and R. Golestanian, *Phys. Rev. E* **85**, 020401 (2012).
 [46] R. Golestanian, T. B. Liverpool, and A. Ajdari, *New J. Phys.* **9**, 126 (2007).
 [47] L. H. Cisneros, R. Cortez, C. Dombrowski, R. E. Goldstein, and J. O. Kessler, *Exp. Fluids* **43**, 737 (2007).
 [48] It has been argued that real swimmers are force free and therefore do not directly feel a Stokes drag. However, the equations of motion can be expressed by a formal force that is proportional to the Stokes drag; see Ref. [60]. Therefore, all scaling relations

- are unaffected by assuming an effective Stokes drag propulsion force.
- [49] S. Kim and S. J. Karrila, *Microhydrodynamics* (Butterworth-Heinemann, Oxford, 1991).
- [50] B. Behkam and M. Sitti, *Appl. Phys. Lett.* **93**, 223901 (2008).
- [51] S. Thutupalli, R. Seemann, and S. Herminghaus, *New J. Phys.* **13**, 073021 (2011).
- [52] Individual surface-tension-driven swimmers have a propagation velocity that scales with the square of the radius [51]. If these droplet particles merge to a larger droplet when clustering, case (a) is realized and this scaling carries over to a cluster such that $v_N \sim R_N^2$. This leads to $\gamma = 0$. However, if the clustering cannot be associated with a merging of the droplet particles, they behave like pushers or pullers. The latter are known to realize case (b) with the scaling $v_N \sim R_N$ [47] and thus again possess $\gamma = 0$ by definition.
- [53] These approximations can be abandoned in a more sophisticated Smoluchowski coagulation equation approach [41], which leads to the same scaling laws. Still, scaling itself is an assumption in the Smoluchowski approach that demands further numerical tests.
- [54] T. Vicsek, A. Czirók, E. Ben-Jacob, I. Cohen, and O. Shochet, *Phys. Rev. Lett.* **75**, 1226 (1995).
- [55] X. Zheng, B. ten Hagen, A. Kaiser, M. Wu, H. Cui, Z. Silber-Li, and H. Löwen, *Phys. Rev. E* **88**, 032304 (2013).
- [56] M. S. Veshchunov, *J. Eng. Thermophys.* **20**, 260 (2011).
- [57] N. Fisher, T. Lewis, and B. Embleton, *Statistical Analysis of Spherical Data* (Cambridge University Press, Cambridge, 1987).
- [58] W. van Saarloos, *Physica A* **147**, 280 (1987).
- [59] M. Lattuada, H. Wu, and M. Morbidelli, *J. Colloid Interface Sci.* **268**, 96 (2003).
- [60] R. Golestanian, *Eur. Phys. J. E* **25**, 1 (2008).